Advances in Soil Science

Food Security and Soil Quality

Edited by
Rattan Lal
B. A. Stewart

CRC Press
Taylor & Francis Group
Boca Raton London New York

CRC Press is an imprint of the
Taylor & Francis Group, an **informa** business

CRC Press
Taylor & Francis Group
6000 Broken Sound Parkway NW, Suite 300
Boca Raton, FL 33487-2742

Printed in the United States of America on acid-free paper
10 9 8 7 6 5 4 3 2 1

International Standard Book Number: 978-1-4398-0057-7 (Hardback)

Library of Congress Cataloging-in-Publication Data

Food security and soil quality / editors: Rattan Lal and B.A. Stewart.
p. cm. -- (Advances in soil sciences)
Includes bibliographical references and index.
ISBN 978-1-4398-0057-7 (alk. paper)
1. Food security. 2. Soils--Quality. I. Lal, R. II. Stewart, B. A. (Bobby Alton), 1932- III. Series: Advances in soil science (Boca Raton, Fla.)

HD9000.5.F5968 2010
338.1'9--dc22 2010002148

Visit the Taylor & Francis Web site at
http://www.taylorandfrancis.com

and the CRC Press Web site at
http://www.crcpress.com

Contents

4 Assessment of Land Degradation, Its Possible Causes and Threat to Food Security in Sub-Saharan Africa

P. L. G. Vlek, Q. B. Le, and L. Tamene

CONTENTS

4.1 INTRODUCTION

The African continent is increasingly recognized as one of the few areas in the world where development is lagging, and it is increasingly attracting the attention of the donor community. With population pressures increasing and low investments in land conservation, the future health of the land is in question (Vlek, 2005). Sub-Saharan Africa (SSA) covers more than 21 million km^2 with an average population density of 30 persons km^{-2} (more than 50% of whom live in cities). Approximately 15% of this land is cultivated and another 4% is mixed forest-cropland. Quantifiable data on the state of these land resources are scarce, even though a Google search yields nearly 2 million hits. The very first of those is a rather sobering paper by Prof. S. C. Nana-Sinkam of the Joint European Commission on Agriculture/Food and Agriculture Organization (FAO) Agriculture Division (http://www.fao.org/docrep/X5318E/x5318e02.htm) that starts out by stating: "Little reliable data are available on the extent of land degradation in Africa. However, anyone who has travelled through the continent has observed that land degradation is widespread, and serious." This gap in our knowledge is hampering land conservation efforts.

Many papers cite widely differing numbers regarding land degradation in Africa. For instance, Reich et al. (2001) claim that about 25% of land in Africa is prone to water erosion and about 22% to wind erosion. GEF (2006) suggests that 39% of the African continent and as much as 65% of the agricultural land are affected by desertification. Such estimates are rarely based on spatially distributed data and fail to identify the regions of concern. Yet, if the scientific community is to help guide investments in land conservation and remediation, it will need to find a way to identify the hotspots of degradation and develop a notion of what is driving the degradation processes of the land in SSA. This means that spatial distribution information showing the relative differences in the magnitude of land degradation across space is necessary.

The Global Assessment of Soil Degradation (GLASOD) (Oldeman et al., 1990; Middleton and Thomas, 1992), which maps land degradation at the global scale, can be considered a first attempt to map land and soil degradation. In preparing GLASOD, 290 national collaborators guided by 23 regional correlators were asked to estimate human-induced decline in land productivity by degree as: light, moderate, strong, or extreme. The national collaborators also were asked to identify the major cause for degradation associated with the respective mapping unit.

Table 4.1 shows the degree of soil degradation as a percentage of the total land area where productivity is reduced by the defined amount of area covered based on the GLASOD survey. When the survey was conducted in the late 1980s, the degree of land degradation in SSA suggested that 83% of the surveyed area was not degraded, 6% was lightly degraded, and 6% was moderately degraded (Table 4.1). The remaining area was considered in worse condition and beyond reclamation, which at 5% seems modest. Yet, no other continent reaches this degree of degradation, and as a percentage of the present arable land area its significance jumps to 25%, assuming that the reported degradation was primarily observed on arable land.

Until recently, the GLASOD map remained the sole source of data on African soil/land degradation. It is, however, a subjective assessment by experts in the late 1980s

TABLE 4.1
Degree of Soil Degradation by Subcontinental Regions

	Severity Class				
	None	Light[a] Low[b]	Moderate[a] Moderate[b]	Strong[a] High[b]	Extreme[a] Very High[b]
Africa (% of total area)					
Middleton and Thomas (1992) (GLASOD)[a]	83	6	6	4	0.2
World (% of total area)					
Middleton and Thomas (1992) (GLASOD)[a]	85	6	7	2	<0.1
Eswaran et al. (2001a, 2001b)	–	12.2	10.5	5.5	6.1
World (1000 km^2)					
Middleton and Thomas (1992) (GLASOD)[a]	110,483	7,490	9,106	2,956	92
Eswaran et al. (2001a, 2001b)	–	14,5999	13,601	7.120	7.91

[a] *Source:* Middleton, N., Thomas, D.S.G., *World Atlas of Desertification*, 1st ed., Edward Arnold, London, UNEP, 1992. With permission.

[b] Data represent the extents of the vulnerability class (for risk assessment of desertification), which is not directly comparable with the severity classes of degraded land given by the GLASOD map (Middleton and Thomas, 1992). *Source:* Eswaran et al., in: Bridges, E. M. et al. (eds.), *Responses to Land Degradation, Proc. 2nd International Conference on Land Degradation and Desertification*, Oxford Press, New Delhi, India, 2001a. With permission. Eswaran et al., in: Stott et al. (eds.), *Sustaining the Global Farm*, 2001b. With permission.

with unknown accuracy. Even though the FAO regularly revisits the GLASOD data, offering more detail (http://www.fao.org/landandwater/agll/glasod/glasodmaps.jsp), most of the basic shortcomings of expert surveys remain. If GLASOD did successfully identify the territories degraded beyond recuperation, it failed to indicate where degradation is in progress and where it may have been abating. Nor did it separate human-induced degradation from climate-related decline.

Advances in satellite remote sensing and the fast development of computing systems have opened up new ways of mapping the magnitude and processes of land degradation over a broad range of geographical scales. In particular, Advanced Very High-Resolution Radiometer (AVHRR) data, from which the Normalized Difference Vegetation Index (NDVI) can be derived, have made it possible to infer land degradation at various scales, and these data have been used extensively (Tucker et al., 1991; Prince et al., 1998; Milich and Weiss, 2000; Weiss et al., 2001; Groten and Ocatre, 2002; Thiam, 2003; Evans and Geerken, 2004; Bai et al., 2008; Hellden and Tottrup, 2008; Vlek et al., 2008). Data series of global coverage, dating back to the early 1980s, are available at no cost. These can be used to gain a long-term and spatially distributed view of the progression of vegetation development over a larger geographical extent.

This chapter builds on the above-mentioned studies and uses the long-term (1982–2003) NDVI data as a proxy to map the spatial distribution of change in net primary productivity (NPP) for SSA. Through a logical analysis of the NDVI trends, the effects of climatic cycles and atmospheric fertilization are accounted for in order to determine the extent to which humans affect NPP. By relating these hotspot areas in SSA with different attributes of the region such as population density, soil/terrain conditions, and land-cover types, it is possible to surmise which underlying processes, for example, deforestation or soil degradation, are at play. To this end, this study analyzes the vegetation dynamics of 320,000 pixels (64 km^2/pixel) at the continental scale. The result of the study is intended to help scientists pinpoint the locations in SSA where more detailed research may be required.

4.2 DEFINITION AND APPROACHES

4.2.1 Definition of Land Degradation

Land is defined as the ensemble of the soil constituents, the biotic components in and on it, as well as its landscape setting and climatic attributes. The most common indicator of the state of the land is its vegetation cover (Safriel, 2007) or, in a more quantitative sense, NPP as a fraction of its potential. In an ecological sense, a loss in biodiversity or ecosystem services with constant NPP would also be a degradation process (Eswaran et al., 2001a). In fact, land degradation sets in when the potential productivity associated with a land-use system becomes nonsustainable, or when the land within an ecosystem is no longer able to perform its environmental regulatory function of accepting, storing, and recycling water, energy, and nutrients (Katyal and Vlek, 2000).

Some natural processes can lead to land degradation, either rapidly (e.g., land slides) or gradually (e.g., climate change), but the phenomenon is mainly due to the interaction of the land with its users and is thus a social problem. Most land degradation is therefore preventable if the underlying causes are understood and acted upon (Eswaran et al., 2001a). The anthropogenic causes of land degradation are related to an ever-increasing demand for food, fodder, fiber, and fuel, as well as shelter and other infrastructure. They include land conversion through land clearing and deforestation, agricultural mining of soil nutrients, and land sealing, irrigation, and pollution.

4.2.2 Approaches to Assess Global/Continental Land Degradation

Until recently, land degradation assessments were often based on the state of soil parameters (Safriel, 2007). Soil conditions often have a close relationship with vegetation cover and (agro-) ecosystem productivity (Figure 4.1), as soil degradation is a common proximate cause of land degradation. Assessing soil degradation at a global, continental, or regional scale is hampered by a shortage of data for long-term quantitative comparisons. At the field scale, it is feasible to develop time series of soil properties that could detect *persistent changes* in soil status (compared to a baseline) required for a valid soil degradation assessment. With current technology, it would be very costly to directly track the dynamics of soil properties over longer time spans at a regional scale. It is practically impossible on a continental or global scale.

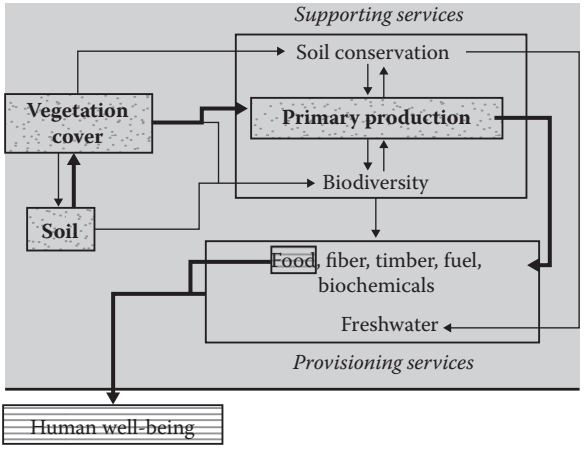

FIGURE 4.1 The state of vegetation cover and soil are direct indicators of the state of land. The state of food provision and human well-being are indirect indicators of the state of land. (From Safriel, U. N., in Sivakumar, M. V. K., and Ndiang'ui, N. (eds.), *Climate and Land Degradation*, Springer Verlag, Berlin, 2007. With permission.)

Monitoring land degradation using remote sensing of NPP is an easier task, especially since satellite imagery has become publicly available. Land degradation expresses itself as reduced biological activity (Reynolds and Smith, 2002; Millennium Ecosystem Assessment, 2005; Safriel, 2007) reflected in aboveground NPP. The most common remote sensing–derived indicator of vegetation productivity is the NDVI, a relative measure of vegetation vigor and photosynthetic activity. NDVI is strongly correlated with NPP and is often used to estimate NPP at regional scales and as a tool for monitoring temporal changes in vegetation (Field et al., 1995; Prince and Goward, 1995). Aboveground NPP (represented by NDVI) has been shown to increase with increasing annual precipitation (Huxman et al., 2004), and indeed correlation studies between rainfall and NDVI have been used to differentiate between human-induced and climate-induced land degradation (Herrmann et al., 2005), where any NDVI trends not explained by rainfall dynamics are ascribed to human actions.

The arguments to use vegetation productivity decline as a proxy for land degradation are twofold. First, NPP of the land is an integrative parameter reflecting many of the ecological functions that deliver ecosystem services for human well-being (see Figure 4.1). Second, a wide variety of remote sensing products are now available, some of them with a record of more than 20 years that reflect the dynamic aspects of the land degradation process. The current remote sensing time series covering Africa are sufficiently long-term and with frequent enough data sampling to allow statistical analysis. Furthermore, combined with global data on climate, topography, soil, land use, and human demographics, the remote sensing data allow further analysis of the underlying causes and processes (Vlek et al., 2008).

One of the meaningful distinctions to be made is between climate-induced and human-induced land degradation, as it is the latter that can be countered by mitigating

strategies. Recent studies use alternative methodologies such as the Residual Trend Analysis (Herrmann et al., 2005) and the trend-correlation–based approach (Vlek et al., 2008) to distinguish the human-induced productivity degradation from rainfall-driven productivity dynamics. These stepwise analyses separate areas where land productivity dynamics are highly correlated with climate change from those where climate does not play a significant role and human-induced degradation is presumed to be dominant. Applied to the Sahelian belt, the results of this method concluded that the reported "greening of the Sahel" over the past 20 years (Olsson et al., 2005; Eklundh and Olsson, 2003; Tucker and Nicholson, 1999; Prince et al., 1998) was largely attributable to improved climatic conditions following the severe drought of the early 1980s.

In some land-degradation studies, use is made of Rain Use Efficiency (RUE), a compound index expressed as NPP per rainfall unit, either alone or in combination with NDVI, particularly for human-induced land degradation in drylands. The idea is that RUE is systematically lower in degraded drylands than in equivalent nondegraded areas (O'Connor et al., 2001), so that despite its wide fluctuation from year to year the long-term RUE trend is considered a good indicator of land degradation. Some scientists even consider RUE a valid indicator for soil degradation, because a decline in RUE appeared to correspond with modeled soil erosion driven by the same rainfall data (Symeonakis and Drake, 2004). However, both a stable system and a change in NDVI proportional to a change in rainfall would yield constant RUE (Safriel, 2007), which is somewhat ambivalent. The strong negative correlation of RUE with rainfall in drylands, for example, for South Africa $r = -0.82$ (Wessels et al., 2007), has been used as an argument against its use. For the purpose of this study, RUE offers little added value.

To analyze the spatiotemporal dynamics of vegetation productivity in SSA in this study, we drew on the NDVI product for a 22-year period spanning from 1982 to 2003 from the Global Inventory Modeling and Mapping Studies (GIMMS), published by the Global Land Cover Facility (GLCF) (http://glcf.umiacs.umd.edu/data/gimms/). The dataset is derived from remote sensing imagery obtained from the AVHRR instrument onboard the National Oceanic and Atmospheric Administration (NOAA) satellite series. The NDVI dataset has been corrected for calibration, view geometry, volcanic aerosols, and other effects that are not related to vegetation change (Tucker et al., 2005). The original data were collected twice monthly on an 8×8 km resolution (pixel size) and were aggregated to obtain the time series of annual mean values as 12-month averages. Average NDVI values for the whole period (1982–2003) of each month were also calculated. These two sets of data were then subjected to statistical analyses to assess variability and trends in vegetation productivity.

4.3 LAND PRODUCTIVITY DYNAMICS IN SSA

A stepwise analysis of the dynamics of the aboveground green biomass in SSA was undertaken that included tests for significance at each step. The process is divided in two phases: (1) mapping a decline in vegetation cover as a proxy for land degradation and (2) interpretation of the mapped degradation. NDVI was used as an NPP predictor at regional scales (Field et al., 1995; Prince and Goward, 1995).

4.3.1 Long-Term NDVI Trend as a Proxy for Change in Land Productivity

In order to evaluate to what extent NDVI can be used to predict NPP across different biomes in SSA, we first analyzed the relationship between annual NDVI and NPP calculated by the Global Production Efficiency Model (1982–2000), obtained from the GLCF at the University of Maryland (http://glcf.umiacs.umd.edu/data/glopem/). A rectangular region containing about 80,950 pixels across different climate zones/biomes in SSA but that excludes the often cloudy areas along the humid coast of the Gulf of Guinea was then selected, and all pixels within that region were used to establish the relationship between NDVI and NPP. Pixels with NPP and/or NDVI near zero (i.e., NPP < 0.5 g C^{-1} m^{-2} yr^{-1} and NDVI < 0.05) were eliminated as they are considered to be too noisy to represent real values (Camberlin et al., 2007). We estimated the NPP-NDVI relationship using six mathematical models: linear, inverse, power, *S*, growth, and exponential functions. The goodness-of-fit assessment revealed that the linear model best fits the sampling data, as it is significant and has the highest prediction capacity:

$$\mathrm{NPP}_i\ (\mathrm{gC\ m^{-2}\ yr^{-1}}) = 1932.517 \times \mathrm{NVDI}_i + 226.530 \tag{4.1}$$

$$(N = 80{,}950\ \text{pixels};\ R^2 = 0.816;\ P < 0.001)$$

The strong relationship between NDVI and NPP reflected in Equation (4.1) agrees with findings in other studies (e.g., Field et al., 1995; Prince and Goward, 1995) and confirms that the AVHRR-NDVI trend can be used as a proxy for land productivity. Whereas NPP is not easy to measure or calculate, NDVI is a simple, satellite-derived index (based on only red and infrared signals), which is readily updated with different remote sensing platforms. The NDVI trend therefore was used in this study as an indicator to assess land degradation across different biomes in SSA.

4.3.2 Rainfall Data and Zones

To assess the relationship between interannual rainfall variability and green biomass (NDVI) in SSA in the absence of well-distributed and continuous station-based rainfall datasets, we used a long-term global gridded climate dataset from the Climatic Research Unit (CRU) of the University of East Anglia (Mitchell and Jones, 2005). The dataset has a spatial resolution of 0.5°, covers the period from 1901–2002, and has been applied and tested in many studies (Fiedler and Döll, 2007). We extracted rainfall data from the CRU dataset version TS 2.1 for the period 1982–2002, and rescaled the original CRU cell size of 0.5° to a cell size of 8 × 8 km to make it congruent with the AVHRR-NDVI dataset. Comparison with the VASClimo Climatology 1.1 (Variability Analysis of Surface Climate Observations) dataset acquired from a different source (Beck et al., 2005) shows very good correlation (Figure 4.2a), which enhanced the confidence in using CRU rainfall data in SSA analysis.

Because the sensitivity of NPP to human interference and rainfall variation is substantially different across biomes (Huxman et al., 2004), a spatial delineation of the major biomes in SSA is needed for land degradation assessment. We differentiated the

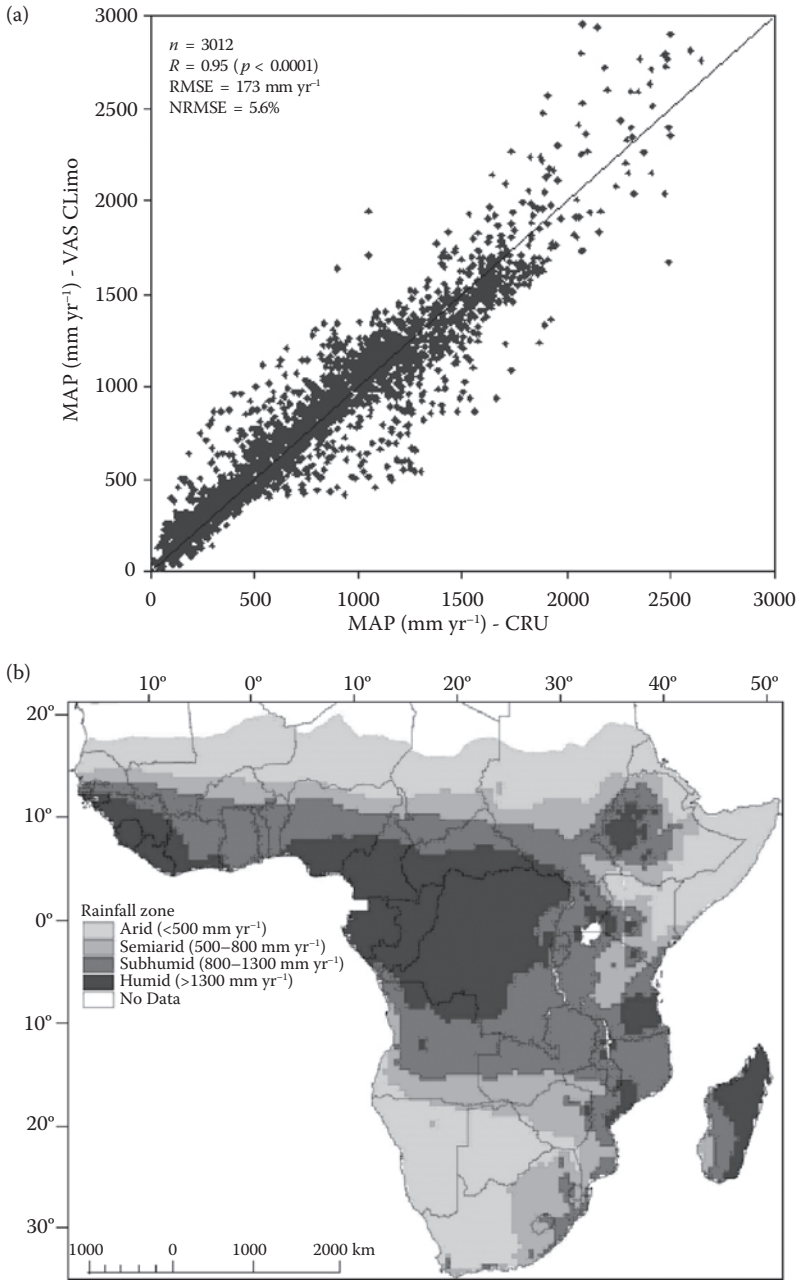

FIGURE 4.2 (a) Correlation coefficient (R) between CRU- and VASCLimo-based MAP for the period 1981–2000 derived for more than 3091 random points across SSA. The normalized root mean squared error is calculated as the root mean squared errors divided by the (MAP_{max}–MAP_{min}) range. (b) Precipitation zones classified using MAP for the period 1981–2002. MAP calculated based on monthly rainfall from the CRU TS 2.1 data. The color map can be directly requested from the authors.

major biomes using mean annual precipitation (MAP) for the period 1981–2002. The SSA was stratified into four precipitation zones: arid (MAP < 500 mm yr^{-1}), semiarid (500 mm $yr^{-1} \leq$ MAP $\leq$ 800 mm yr^{-1}), subhumid (800 mm $yr^{-1} \leq$ MAP $\leq$ 1300 mm yr^{-1}), and humid (MAP > 1300 mm yr^{-1}) (Figure 4.2b). The boundaries of these precipitation zones were selected such that they agree with the main agroclimatic zones for Africa. Compared to the most recent Köppen-Geiger climate map (Kottek et al., 2006), the Arid and Semiarid zones in Figure 4.2b more or less match the arid and semiarid climates (BW and BS classes), the Subhumid zone overlays the tropical dry-wet (savannah) climate (Aw class), and the Humid zone matches the humid equatorial climate (Af and Am classes).

4.3.3 Vegetation Response to Shifts in Annual Rainfall

Spatial and temporal differences in NDVI are closely related to climate or climate change in many environments (Eastman and Fulk, 1993; Ichii et al., 2002; Nicholson et al., 1990). In an attempt to disentangle human-induced and climate-driven vegetation productivity dynamics, the correlation between interannual vegetation productivity (expressed as NDVI) and rainfall across SSA over the 21-year period was assessed using Pearson's correlation coefficient for the period 1982–2002 for all 320,000 pixels mapped in Figure 4.3a. The area where vegetation productivity correlates positively with rainfall changes (positive values in Figure 4.3a) covers the Sahelian band and the semidesert regions of southern Africa. The areas with the negative Pearson's coefficient (negative values in Figure 4.3a) stretch along the subhumid band from Southern Chad to the Casamance of Senegal. The nonresponsive areas are found in the high-rainfall zones where the variation of rainfall is limited, or in the very dry zones where the variation is too high to yield significant trends. The depicted spatial pattern of NDVI response to interannual rainfall in SSA agrees largely with the result given by Camberlin et al. (2007) and Hellden and Töttrup (2008).

To be considered in this analysis, the correlation between the interannual NDVI and rainfall had to not only be significant ($P < 0.05$) but also greater than 0.5 or less than –0.5. In areas where, by these criteria, precipitation increases over the past 20 years had led to improved biomass (NDVI) signals (positive in Figure 4.3b), human effects on vegetation productivity are possibly masked. A significant negative correlation (negative in Figure 4.3b) can reflect two different responses: (1) where rainfall goes up whereas the vegetation cover declines due to severe degradation, areas of particular concern, or (2) where rainfall goes down but vegetation goes up due to human interventions such as the establishment of exclusion zones, afforestation, or irrigation schemes.

4.3.4 Long-Term Trend in Land Productivity in SSA

The trend of NPP of the land in SSA over 1982–2003 was statistically analyzed for every pixel using the annualized NDVI data. The net change in NDVI per year (dNDVI yr^{-1}) was measured by the slope coefficient (A) in the linear relationship: NVDI = $A \times$ Year + β, where β is the intercept. If the beginning year (1982) was set to zero, β indicates the initial state of NPP for a pixel. The A values are mapped in Figure 4.4a. The NDVI slope of every pixel was tested for statistical significance

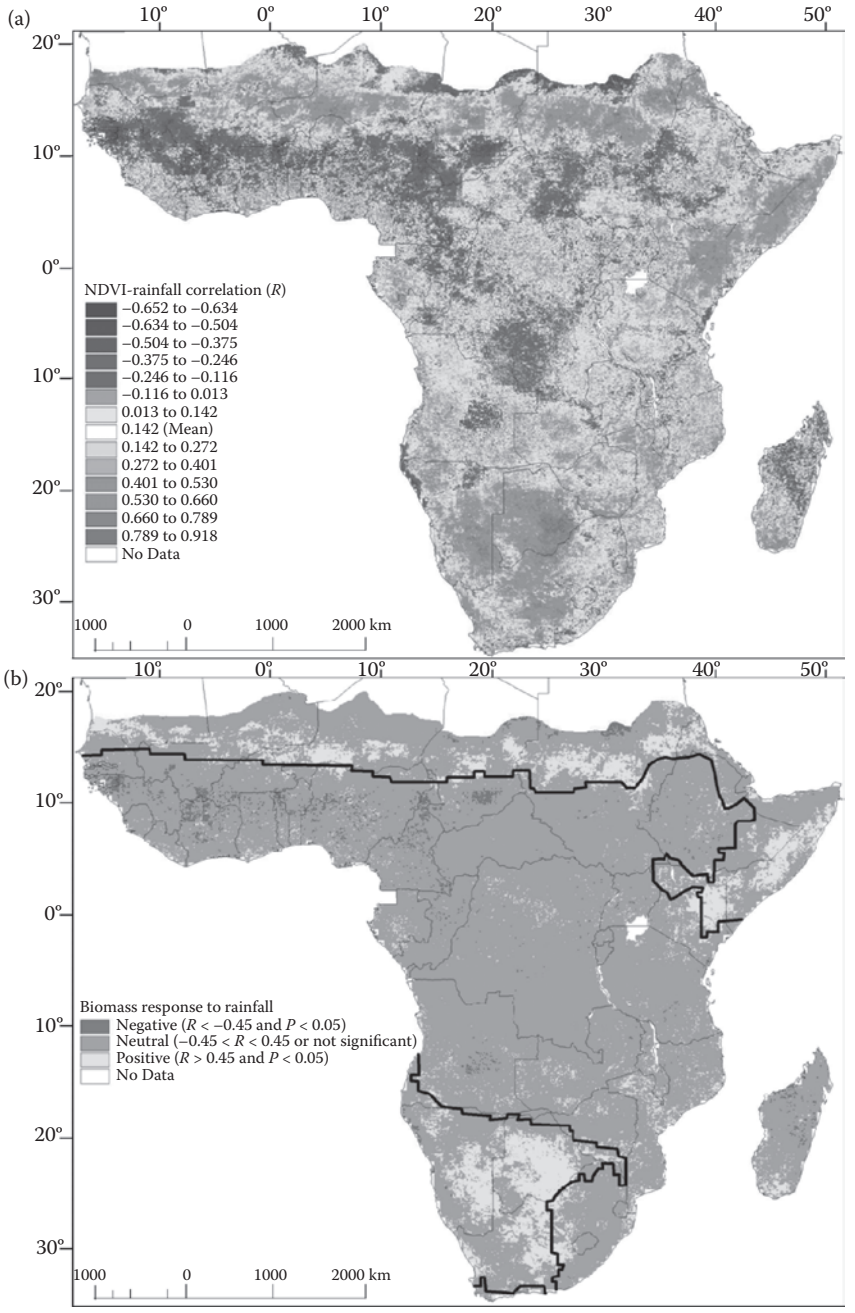

FIGURE 4.3 (a) Pearson's correlation coefficient (R) between annual NDVI and rainfall for the period 1982–2002. (b) Areas of different modes of long-term vegetation productivity response to interannual rainfall based on NDVI-rainfall correlation analysis. Bold black lines represent the 500 mm yr^{-1} isohyets averaged for the same period. The color maps can be directly requested from the authors.

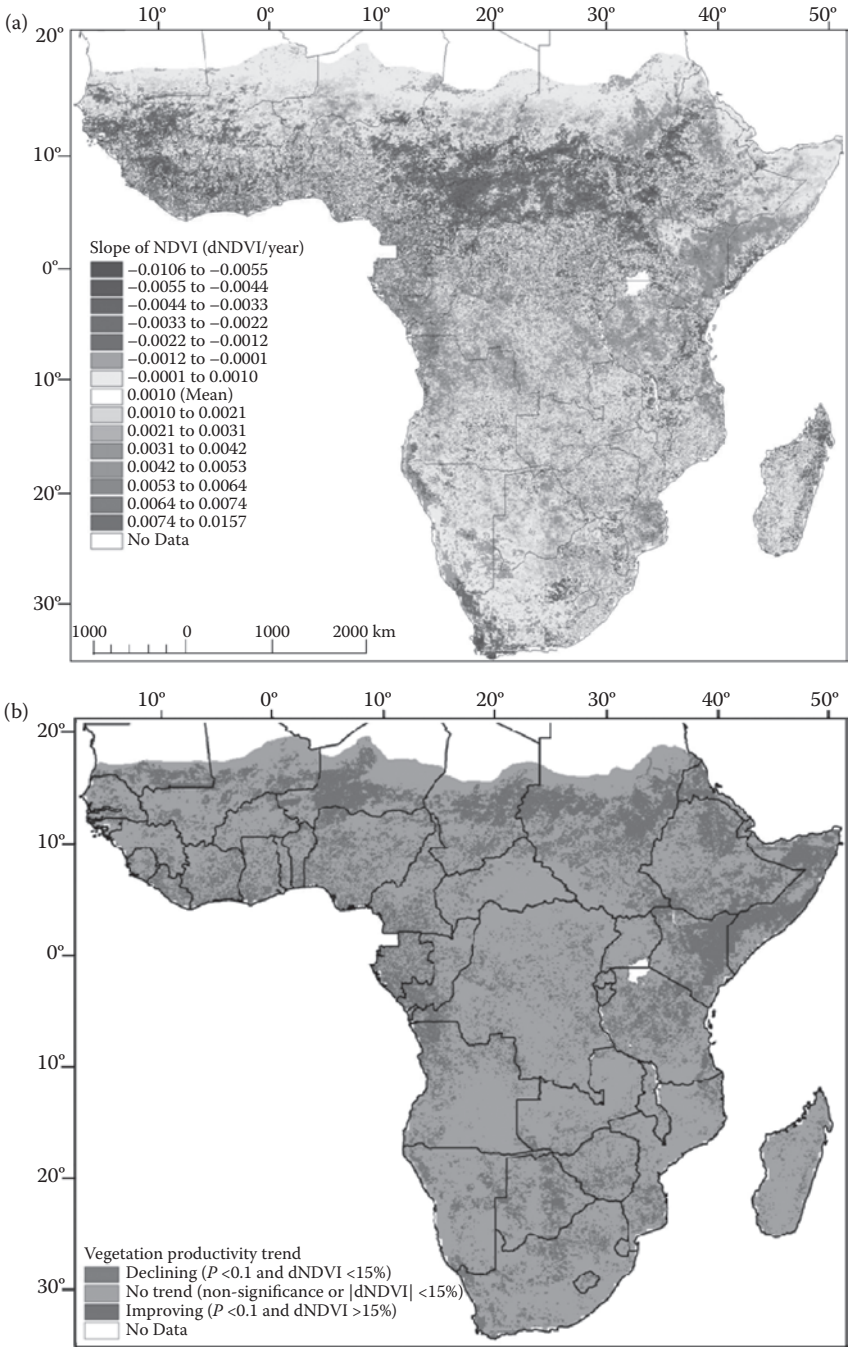

FIGURE 4.4 (See color insert following page 82.) (a) Slope coefficient (*A*) of interannual NDVI over the period 1982–2003. (b) Extent of long-term vegetation productivity trend (1982–2003) of SSA with confidence level of 90% and relative productivity change of at least 15% over the past 22 years.

against the stable baseline. Given the very dynamic nature of human interference in vegetation dynamics, we accepted the somewhat relaxed confidence level of 90% to be significant in the trend analysis. We subsequently tested different threshold values of change in comparison to the baseline (1982 NDVI) and mapped those pixels with a significant change ($P < 0.10$) of 15% or more over 22 years. Figure 4.4b shows the geographic extent of productivity shifts as compared to that in 1982 meeting these criteria. The map shows that some of the most significant changes in NDVI are found in areas of low primary productivity. These areas lie in the drier parts of SSA, where NDVI values are very small to begin with. In such dry biomes, small changes in absolute NDVI values constitute large changes in relative terms.

Based on the 15% threshold, the area with sustained decline in vegetation over the observation period of 22 years amounts to 0.54 million km^2 (about 2.5% of the SSA landmass), whereas about 4.38 million km^2 (20.5% of the SSA) exhibit a significant improvement in vegetation productivity. Thus, the areas of significant productivity decline are only a fraction of the areas of improving productivity.

The extent of the areas with declining, improving, or stable NDVI in the arid, semiarid, subhumid, and humid zones is given in Table 4.2. The largest area with declining productivity is found in the subhumid tropics, considered the breadbaskets of SSA. A large proportion of the area with improving NDVI is found in the arid zone, such as the Sahelian and Horn of Africa regions as well as in parts of Botswana, as demarcated in Figure 4.4b. These areas largely coincide with areas where the vegetation is responsive to interannual rainfall variation (positive in Figure 4.3b), and the increase in NDVI is likely due to a gradual improvement in annual precipitation. This phenomenon has been reported in the literature as the "greening of the Sahel" (Olsson, 1993; Prince et al., 1998; Tucker and Nicholson, 1999; Eklundh and Olsson, 2003; Olsson et al., 2005; Hellden and Töttrup, 2008). The early 1980s indeed experienced a long-term drought. However, since these areas also lay below the 500-mm isohyets, averaged for the 1982–2002 period, they are

TABLE 4.2
Area (km^2) of Different Biomass Trends in Different Climate Zones

	Area (km^2)				
Land with Productivity Trend	**Arid (<500 mm yr^{-1})**	**Semiarid (500–800 mm yr^{-1})**	**Subhumid (800–1300 mm yr^{-1})**	**Humid (>1300 mm yr^{-1})**	**Total**
Declining	106,370 (0.50)	131,960 (0.61)	233,350 (1.09)	70,650 (0.33)	542,330 (2.54)
Neutral	4,476,230 (20.93)	2,718,910 (12.71)	5,233,350 (24.47)	4,031,880 (18.85)	16,460,360 (76.97)
Improving	2,197,060 (10.27)	743,290 (3.48)	733,250 (3.43)	708,540 (3.31)	4,382,140 (20.49)

Note: Numbers within parentheses are the percentage of the total SSA landmass (total = 21.38 million km^2).

of limited agricultural importance. Pastoralists that occupy these lands and are a vulnerable group should have benefited from this improvement.

The improvement in vegetation productivity in the wetter areas (10.2% of the SSA landmass) is not related to increasing rainfall, because no such correlation could be established (Figure 4.3b). It is also not possible to attribute such improvement to human management and/or expansion of irrigation practices because the areas of improved biomass cover too large a geographical region. The greening of these wide areas will need to be explained by a plausibly natural phenomenon.

4.3.5 Atmospheric Fertilization Effect on NPP

The greening of extensive areas in SSA is most likely attributable to a change in atmospheric composition. This positive response of vegetation productivity to rising levels of atmospheric CO_2 due to a stimulation of photosynthesis has been well documented (Grace et al., 1995; Körner, 2000; Nowak et al., 2004; Norby et al., 2005; Boisvenue and Running, 2006). Furthermore, it has been observed that the increasing NO_x load of the atmosphere over SSA is causing an increase in reactive nitrogen (N) deposition and enhances carbon sequestration (Galloway et al., 2004; Adam et al., 2005; Hagedorn et al., 2005; Dentener, 2006; Magnani et al., 2007; Reay et al., 2008; LeBauer and Treseder, 2008). Atmospheric fertilization at a rate of 0.63 ± 0.31 Mg ha^{-1} yr^{-1} over the past four decades was recently also reported for closed-canopy tropical forest sites in Africa (Lewis et al., 2009).

The actual change in vegetation productivity ($dNDVI_{act}/dt$ = slope coefficient A) can be considered the net balance between the partial changes caused by human activities ($dNDVI_{human}/dt$) and those caused by natural processes ($dNDVI_{natural}/dt$) as shown below:

$$dNDVI_{act}/dt = dNDVI_{human}/dt + dNDVI_{natural}/dt \tag{4.2}$$

Positive values for $dNDVI_{natural}/dt$ can be due to environmental change such as improved rainfall or atmospheric fertilization, and positive values for $dNDVI_{human}/dt$ can be related to afforestation, exclusion zones, or soil remediation. Having excluded the areas with rainfall-related increases in NDVI (Figure 4.3b), we sought to quantify the effect of atmospheric fertilization on the dynamics of vegetation productivity over time. To this end, we selected the pristine areas across SSA with (1) little human habitation, (2) no significant NDVI-rainfall correlation, and (3) an increasing NDVI (Table 4.3). For the period 1982–2002, this resulted in 20,000 pixels (about 1.3 million km^2). The rate of NPP improvement for these areas as expressed in the average NDVI slope ($dNDVI_{act}/dt = A$) was ascribed to atmospheric fertilization. The baseline slope values of biomass accrual in those pristine lands for each climate zone were subsequently used as a new baseline to recalculate the trend of NDVI over the 22-year period.

Recalculation of the time series of NDVI decline ($dNDVI_{human}/dt$) by correcting for atmospheric fertilization results in a substantial increase in the number of pixels that experience land degradation processes. Vlek et al. (2008) estimated that 10% of SSA was significantly affected by degradation as reflected in a decline in

TABLE 4.3
Increasing NDVI Trends in Areas of Low Human Population and No Significant Correlation between NDVI and Rainfall (see Figure 4.5 for the Related Geographic Extent)

Precipitation Zone	Spatial Average of NDVI Slope (*A*)	Area (km^2) of Different NDVI Trends
Arid	0.0012	686,470
Semiarid	0.0025	144,390
Subhumid	0.0028	178,250
Humid	0.0036	269,950
Total		178,250

NDVI (Figure 4.4b). Based on the current analysis, 27% of the land is subjected to degradation processes, but most of this is masked by atmospheric fertilization and does not show up directly in a decline in NDVI (Figure 4.5). In these areas, land-degrading processes such as soil degradation, excessive grazing, or wood harvesting were (more than) compensated by the increased vegetation vigor due to atmospheric CO_2 and NO_x, and thus go undetected with simple NDVI tracking.

The geographic spread of the area subject to human-induced degradation processes (Figure 4.5) among the different climatic zones of SSA is provided in Table 4.4. Pixels with significantly declining $dNDVI_{human}/dt$ amounting to 15% or more are found in all rainfall zones although somewhat less in the semiarid tropics. For 14.3% of the 5.94 million km^2, 14.3% of the decline in $dNDVI_{human}/dt$ takes place despite an improving trend in precipitation (labeled Negative in Table 4.4), which is of particular concern.

The GLASOD survey, which is based on "expert ground observations," concluded that in the early 1980s about 10% of SSA experienced serious human-induced land degradation (Middleton and Thomas, 1992). The areas identified in the survey appear to have reasonable correspondence with Figure 4.5. Bai et al. (2008) used a rain-use efficiency adjusted NDVI to map the global land degradation trend, and their result shows that about 26% of SSA experiences land degradation, but the geographic correspondence with Figure 4.5 is limited. Hellden and Tottrup (2008) applied NOAA AVHRR NDVI for desertification monitoring, and their result shows an extensive greening in the majority of the world's dryland regions. Future studies will be needed to ground-truth these satellite-based assessments.

4.4 RELATIONAL ANALYSIS OF LONG-TERM LAND PRODUCTIVITY DECLINE

In the following section, the areas of human-induced land productivity that decline in the long term (Table 4.4) are related to some of the other attributes of the land that are stored in databases held by different organizations. Such analyses may provide

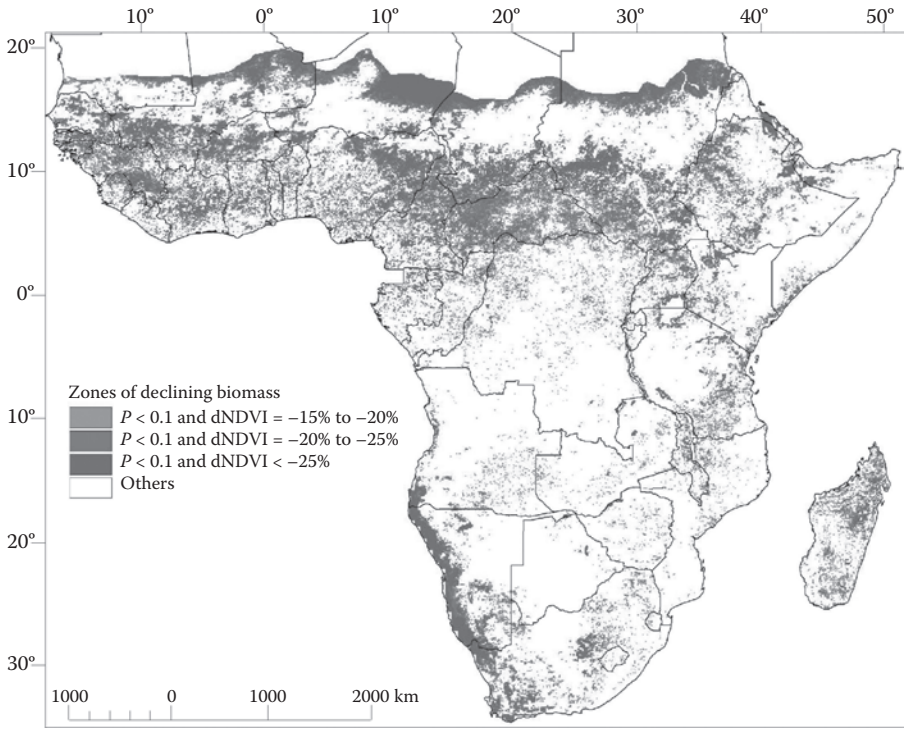

FIGURE 4.5 Geographic extent of areas in SSA noticeably affected by land degradation processes (declining $dNDVI_{human}/dt$) over the period 1982–2002 when taking into account atmospheric fertilization. The color map can be directly requested from the authors.

spatially explicit insights in the likely processes leading to land degradation, offering guidance on mitigation or adaptation. It is recognized that the value of such analysis is directly related to the quality of the respective databases, which for SSA are often deficient. However, the logical framework retains its validity and can be easily reapplied whenever better data become available.

4.4.1 Population Factor

If human factors are of key importance in land degradation (Abubakar, 1997; Eswaran et al., 1997; Reich et al., 2001), areas of degradation would likely be associated with high population pressure, as was suggested by the GLASOD analysis. The mean population densities for the 1980–2000 period (average of 1980, 1990, and 2000) were obtained from the Grid Population of the World Version 3 (GPWv3) dataset of the Center for International Earth Science Information Network at Columbia University and Centro Internacional de Agricultura Tropical (CIAT) (Balk and Yetman, 2004).

The mean population densities for the four climatic zones are 8 persons km^{-2} for the Arid zone, and 25, 32, and 28 persons km^{-2} for the Semiarid, Subhumid,

TABLE 4.4
Areas (km²) with Significant $dNDVI_{human}/dt$ and an Overall NDVI Decline from the Baseline of 15%, Subject to Human-Induced Degradation Processes

Climatic Region	Correlation with Rainfall	Area (km²)	% of Total Area
Arid	Negative	252,480	4.25
Arid	Neutral	1,592,380	26.82
Semiarid	Negative	169,530	2.86
Semiarid	Neutral	808,760	13.62
Subhumid	Negative	277,830	4.68
Subhumid	Neutral	1,405,440	23.67
Humid	Negative	146,560	2.47
Humid	Neutral	1,257,090	21.17
Total area subjected to human-induced degradation process		5,910,070	99.54

[a] The remaining percentage is losing productivity because of the reduction in annual rainfall and is thus considered not human-induced.

and Humid zones, respectively. The pixels in these rainfall zones that show signs of vegetation productivity decline (Table 4.4) have average population pressures of 4, 32, 31, and 32 persons km^{-2}, respectively, close to those for the rainfall zones as a whole. To see how the population is distributed within the degrading zones, each of the degrading pixels of the respective rainfall zones was differentiated according to three classes of population density (smaller than the mean, more than twice the mean, and between these two). For the Arid zone, these ranges would thus be <4, 4–8, and >8 persons km^{-2}.

The map in Figure 4.6 clearly shows that in each climatic zone, the areas most affected by degradation processes are those low in population density. These regions possibly constitute marginal or fragile lands with limiting carrying capacities that are easily overpopulated. Food security in such areas will be threatened as population density continues to increase unless measures are taken to increase the carrying capacity of these regions and reverse degradation or to reduce the pressure on the land by offering alternative employment and means to purchase food. However, there are also some areas where vegetation decline is strong and population density is high, notably southwestern Ethiopia, the Ugandan highlands, northern Nigeria, and southeastern Sudan. These higher population densities are found on the better and more productive land, and degradation problems in these areas should be addressed with priority. In case nutrient depletion is the cause, these areas could be targeted with fertilizer marketing schemes, as inputs are likely to be economical in such regions (Kaizzi et al., 2006). In the case of erosion, investments would be needed to slow runoff and restore land (Tamene et al., 2006).

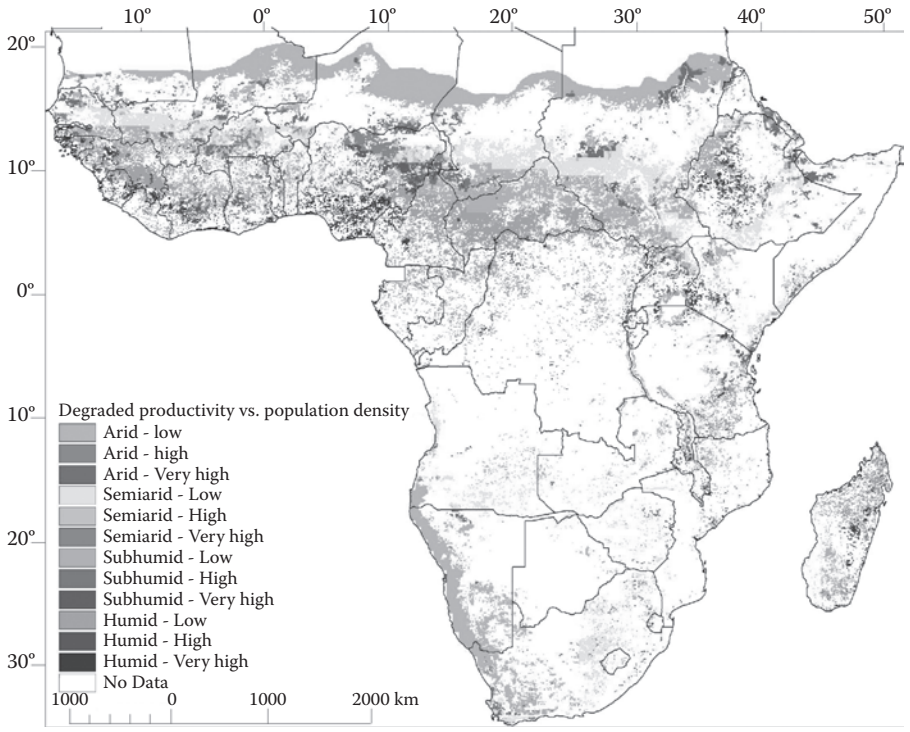

FIGURE 4.6 **(See color insert following page 82.)** Land affected by productivity decline ($dNDVI_{human}/dt$) in different climate zones that is not attributable to reduced annual rainfall in relation to population density (Low, High, and Very high categories) showing most of the declining zones to be with relatively low population density.

4.4.2 NDVI Decline in Relation to Soil and Terrain Constraints

Topography affects climatic conditions, regulates water flows, and determines landscape and soil patterns (Gessler et al., 2000; Wilson and Gallant, 2000; Park et al., 2001), and thus affects vegetation cover. Furthermore, soil quality is closely interlinked with the primary productivity of standing vegetation (Safriel, 2007). Thus, the pattern of primary productivity decline as it relates to soil and terrain conditions may offer some insight in what processes are involved.

SSA was differentiated according to the topographic and soil-based suitability of the land for agriculture using FAO and United States Geological Survey (USGS) databases. Soil constraint classes were derived from the FAO classification of soil constraints (Fischer et al., 2002) by aggregation as follows: Good (FAO class 1 or 2), Bad (FAO class 3 or 4), and Unsuitable (FAO class 5, 6, 7, or 8).

Topographic SRTM (Shuttle Radar Topography Mission) elevation data with a pixel resolution of 1 km derived from USGS (2004) were used to derive terrain constraint with respect to agriculture productivity. Pixels with elevation >3500 m above sea level (a.s.l.) or surface slope >25° were considered not suitable for agriculture

(Sheng, 1990). The following categories were delimited: Good ($0° \leq$ slope $\leq 15°$ and elevation ≤ 3500 m a.s.l.), Bad ($15° <$ slope $\leq 25°$ and elevation ≤ 3500 m a.s.l.), and Unsuitable (slope $> 25°$ or elevation > 3500 m a.s.l.).

The area affected by human-induced degradation processes resulting in negative $dNDVI_{human}/dt$ (Table 4.4) was mapped by classifying each pixel according to terrain and soil suitability for agriculture as shown in Figure 4.7. Of the 5.91 million km^2 that were considered subject to degradation processes, the areas unsuitable for agriculture because of topographical or soil constraints comprise about 1.72 million km^2, 1% of which was constrained by both topography and soil conditions. Most of these pixels are found in regions with relatively low population density, as they likely pose inherent restrictions on exploitation and habitation (Table 4.5). Erosion from degrading areas with unsuitable terrain can cause damage to reservoirs and agricultural land downstream. Such areas should remain under protective vegetation and, if not already so, should be revegetated in order to protect food production downstream.

About 4.2 million km^2 of the area noticeably subject to degradation processes (Table 4.4) are potentially cultivable land and cover a band that extends from West Africa to Ethiopia (Figure 4.7), the breadbaskets of Africa. Nearly 50% of this region is on good soils that are very likely under cultivation and probably experience soil

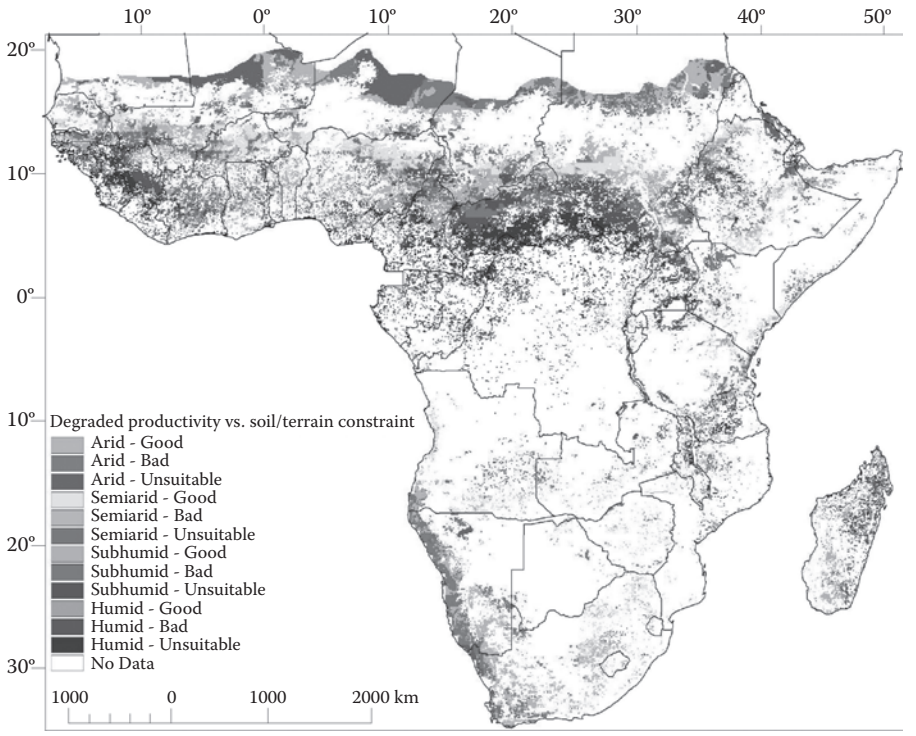

FIGURE 4.7 Extent of land subject to human-induced land degradation processes (negative $dNDVI_{human}/dt$), differentiated according to soil and terrain constraint classes (Good, Bad, and Unsuitable categories). The color map can be directly requested from the authors.

TABLE 4.5
Area (km²) of Land Exhibiting Negative $dNDVI_{human}/dt$ Due to Land-Degradation Processes, with Differential Soil/Terrain Constraints

		Soil/Terrain Constraint		
Population Density	**Total Area (km²)**	**Good**	**Bad**	**Unsuitable**
		Arid		
Low density	1,540,992	666,304	505,152	369,536
High density	91,200	39,168	26,368	25,664
Very high density	212,672	111,616	61,376	39,680
		Semiarid		
Low density	733,376	272,384	302,848	158,144
High density	119,936	55,744	45,376	18,816
Very high density	124,992	67,008	41,216	16,768
		Subhumid		
Low density	1,262,720	398,400	474,240	390,080
High density	212,096	93,888	72,576	45,632
Very high density	208,448	101,248	70,080	37,120
		Humid		
Low density	1,125,440	248,896	334,656	541,888
High density	116,672	37,760	37,376	41,536
Very high density	161,536	71,424	54,208	35,904
Total	5,910,080	2,163,840	2,025,472	1,720,768

degradation. More than 50% of this region, however, is on poor-quality soils. Some of these areas are likely also under cultivation and, if economical, might benefit from soil remediation programs. In the case of pastures and forests, overexploitation for short-term gains (deforestation, overgrazing) should be discouraged.

4.4.3 Land Use and Land-Degradation Processes

Additional information might be gained from knowing the land use of the areas that experience negative human impact. For instance, in the forest regions human interference most likely involves excessive wood harvesting, whereas in agricultural areas it is more likely to be related to soil-nutrient mining. The map depicting land affected by soil degradation processes (Figure 4.5) was cross-referenced with the land-use/cover map of GLC2000 (Mayaux et al., 2004), allowing differentiation of the areas subject to land-degrading processes according to land-use type. The GLC2000 dataset is based on Satellite Pour l'Observation de la Terre vegetation data with 1-km resolution. The quality of the map has been verified using different approaches and using data from a spectrum of sources such as ground observations, national forest statistics, previous land-cover maps, and high-resolution satellite imagery (Achard et al., 2001; Bartalev et al., 2003; Cihlar et al., 2003; Fritz et al., 2003; Mayaux et al.,

2004). The map's quality has also been compared with that of other global land-cover maps (e.g., Giri et al., 2005).

Combining the GLC 2000 dataset with the GIMMS-derived information summarized in Figure 4.5 yielded the regions affected by human-induced land-degradation processes under different land cover/use. The statistical details are shown in Table 4.6. In total, about 27.6% of the SSA region (5.91 million km^2) is suffering from a significant human impact on primary productivity as measured against the baseline corrected for atmospheric fertilization. Of the 1.72 million km^2 that are not suitable for agriculture (Table 4.6), 288,000 km^2 are actually being farmed (forest cropland or agriculture) but probably should not be. In the dry areas, this is agricultural land, whereas in the more humid regions these are the forest-cropland mosaics. Means should be found to offer these farmers alternatives to ensure their food security so that land can be restored over time, for example, by establishing exclusion zones.

Of the remaining 4.19 million km^2 that experience a negative human impact, 0.97 million km^2 are actually farmed (agriculture and forest/cropland mosaic) and are likely overexploited or poorly managed. The area is equally divided between land with good soils and land with bad soils, except in the humid forest/cropland zone where the bad soil/terrain areas appear to be under threat. These agricultural regions require more sustainable farming practices. Thus, in all, about 1.25 million km^2 of cultivated land are experiencing some degree of human impact.

As shown in Table 4.6, about 0.95 million km^2 of the area under grassland, largely in the arid and semiarid areas, show a human impact on productivity, probably due to overgrazing. This area constitutes only 17% of the 5.6 million km^2 of grassland in SSA, but more than 75% of which (0.78 million km^2) are found in the dry (arid and semiarid) areas, home to some of the most vulnerable communities, where the people depend on livestock grazing for food security.

In the subhumid tropics, the woodlands/shrublands are the most affected because they are predominant there, whereas the mosaic forest/savanna and dense forests are threatened in the humid areas. As much as 28% of the woodlands/shrublands in SSA is subjected to significant human-induced degradation processes, probably reflecting encroachment by farmers on these natural habitats. For the expansive, more densely forested regions, the area with vegetation affected by human impact covers only 13.8% of the region, most of which is unsuitable for agriculture. This may be a region of intensive deforestation.

Figure 4.8 provides an overview of the areas of declining agricultural productivity. The affected farming communities stretch across SSA from West Africa to Ethiopia. The cultivated areas (category "Suitable soil/terrain - Cultivated" in Figure 4.8) are most likely land experiencing a declining resource base due to soil degradation, for example, declining soil organic matter, erosion, or soil mining. Food security is becoming increasingly threatened in such areas. Also indicated in Figure 4.8 are regions that are considered unsuitable for agriculture but are, in fact, being cultivated (category "Unsuitable soil/terrain - Cultivated" in Figure 4.8). The latter are found, for instance, on the eastern borders of Sierra Leone and Liberia, eastern Nigeria, as well as in Uganda. Cultivating such land is likely not sustainable and will increasingly lead to food insecurity. Such areas should probably be rehabilitated to their natural conditions. Finally, there are areas that are experiencing human impact and have

TABLE 4.6

Areal Extent of Land that Experienced a Negative Human Impact in 2000, as a Function of Land Use/Cover Types Calculated for Each Composite Climatic Zone across Soil/Terrain Constraints

		Area Land Use/Cover Type (km^2)							
Climate	**Soil/Terrain Conditions**	**Defense Forest**	**Forest/ Savanna**	**Forest/ Cropland**	**Woodland/ Shrubland**	**Grassland**	**Agriculture**	**Others**	**Total Area (km^2)**
Arid	Good soil/terrain	512	64	0	4,352	311,744	27,264	472,000	815,936
	Bad soil/terrain	448	0	0	5,504	167,808	23,232	395,392	592,384
	Unsuitable soil/terrain	192	64	0	1,728	61,760	10,624	362,176	436,544
Semiarid	Good soil/terrain	7,488	320	0	51,968	123,456	205,248	3,008	391,488
	Bad soil/terrain	2,624	64	64	82,432	97,152	207,040	2,816	392,192
	Unsuitable soil/terrain	576	128	64	43,712	19,392	122,816	7,936	194.624
Subhumid	Good soil/terrain	24,960	5,056	21,696	327,040	48,832	147,840	5,440	580,864
	Bad soil/terrain	28,864	17,280	29,568	370,240	29,460	139,520	7,488	622,720
	Unsuitable soil/terrain	17,664	11,904	14,912	315,584	8,960	63,552	47,104	479,680
Humid	Good soil/terrain	70,912	29,760	46,336	128,192	41,408	26,752	2,304	345,664
	Bad soil/terrain	123,456	48,064	74,624	138,880	26,240	19,136	3,840	434,240
	Unsuitable soil/terrain	187,968	163,648	66,496	163,776	14,656	10,048	17,152	623,744
Total area with human impact		465,664	276,352	253,760	1,633,408	951,168	1,003,072	1,326,656	5,910,080
Total area within SSA		3,370,304	676,928	808,320	5,729,728	5,559,680	3,211,840	2,323,648	21,680,448

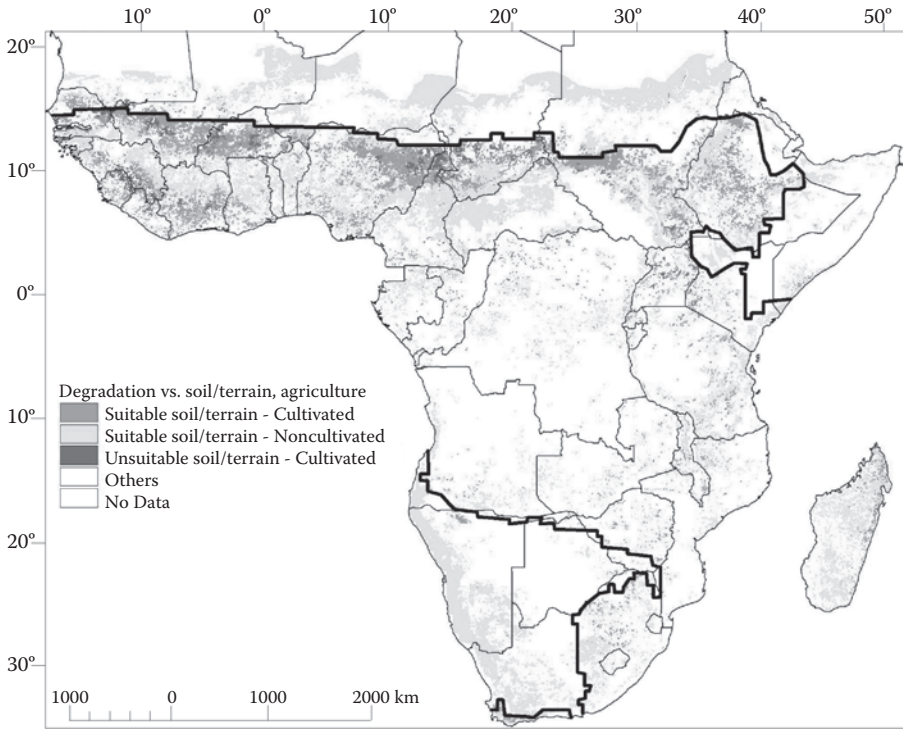

FIGURE 4.8 Arable areas with biomass productivity negatively impacted by human activity as a function of their agricultural use and soil/terrain constraints. Note that none of the NDVI of these pixels exhibited a positive correlation with interannual rainfall. Suitable soil/terrain includes Good and Bad soil/terrain conditions as in Figure 4.7. Cultivated land includes Forest/Cropland and Agriculture categories of Table 4.6. The color map can be directly requested from the authors.

agricultural potential (category "Suitable soil/terrain - Noncultivated" in Figure 4.8), provided they receive adequate rainfall. The declining NDVI signal in these zones may be reflecting gradual conversion of land. Whether this process is desirable given the current concern about climate change is open for debate (Vlek et al., 2003).

Detailed information is easily lost when 320,000 pixels are mapped on 10 × 10 cm. However, details can be obtained by consulting the electronic map versions (http://www.zef.de).

4.5 LAND DEGRADATION AND THE THREAT TO FOOD SECURITY

Excessive pressure on land is the prime cause of human-induced degradation of agricultural land. Imhoff et al. (2004a) expressed this pressure as the human appropriation of net primary productivity (HANPP). Mapping HANPP as a percentage of NPP for each pixel gives a spatial balance sheet of NPP "supply" and "demand" by the local population. In general, pixels with higher HANPP (% of NPP) would

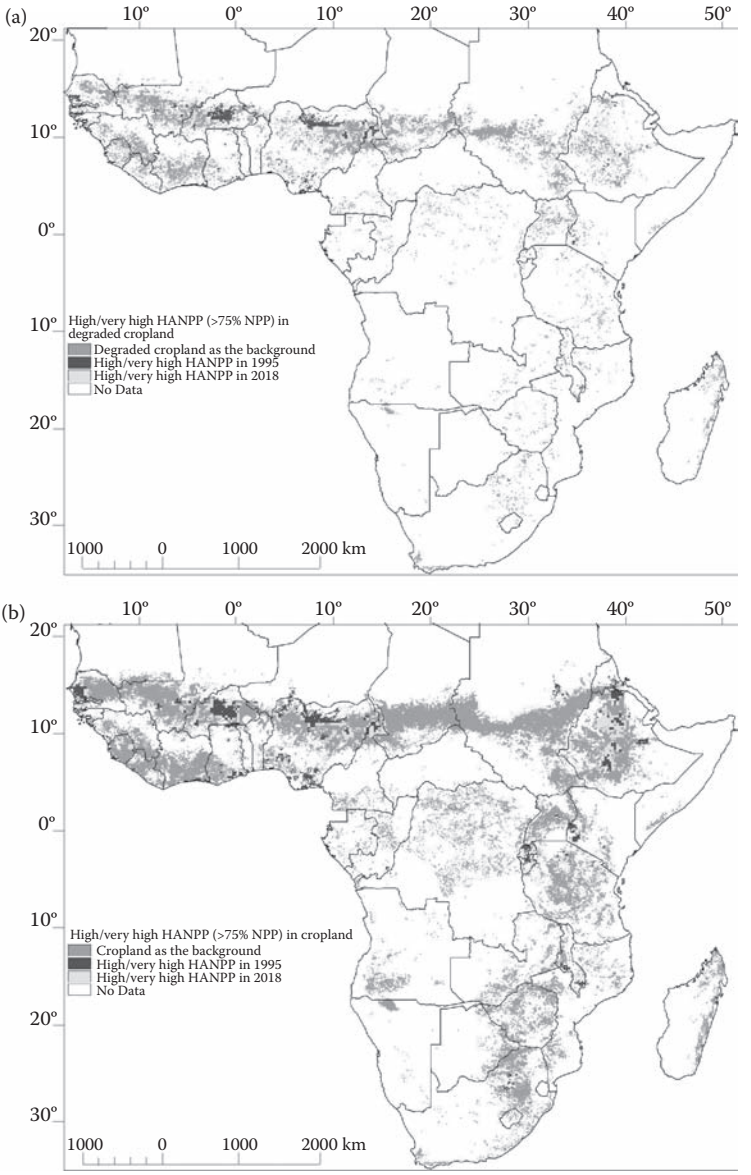

FIGURE 4.9 (a) Human pressure on degraded cropland (gray) expressed in HANPP (% of in situ NPP) in 1995 (dark gray) (extracted and reclassified from Imhoff et al., Human Appropriation of Net Primary Productivity as a Percentage of Net Primary Productivity, Socioeconomic Data and Applications Center, 2004b; with permission) and projected to 2018 (light gray). (b) Same as (a) but for all of the agricultural land in 2000. Note: $HANPP_{2018}$ (% of NPP) = $HANPP_{2018} \times 100/NPP_{2018}$, where $HANPP_{2018}$ is estimated based on population growth rate (3%) and the HANPP in the base year (1995): $HANPP_{2018} = HANPP_{1995}$ $(1 + 0.03)^{22}$, and NPP_{2018} is predicted using the annual NDVI slope and the base NPP in 1995 of Figure 4.4b. The color maps can be directly requested from the authors.

leave a greater footprint of human consumption with commensurate environmental impact. Imhoff et al. (2004a) produced a global HANPP map (resolution of 0.25°).

Because NPP represents the primary food energy source for the world's ecosystems (Imhoff et al., 2004a), the persistent decline in NPP reduces the ability of the land to provide food for human consumption. Food insecurity can be brought about by a decline in NPP or an increase in population or by both. For Africa as a whole, Imhoff et al. calculated an HANPP of 12.4% for 1995, suggesting a light impact of human consumption overall. However, the spatial distribution of HANPP for SSA (Imhoff et al., 2004b) reveals a great spread from 0% to more than 100% with an average of 16%. The cultivated area (Figure 4.9b) of the subcontinent consumes 27% of NPP, in the degraded land as much as 32% on average (Figure 4.9a), and this biomass is mainly appropriated for food products. The areas where excessive fractions of NPP are appropriated for human agricultural production are concentrated in a belt running through Mali, Burkina Faso, Niger, and Northern Nigeria, areas often in the news because of food insecurity.

Anticipating the changes in the appropriation ratio (HANPP) offers a view of where food insecurity may emerge as an issue in the future. Using the change in NDVI as a proxy for the shift in NPP (Figure 4.4b) and assuming a continued population growth of 3% yields a spatial distribution of HANPP, represented for 2018 in Figure 4.9 (category "High/very high HANPP in 2018"). The areas bordering the Sahel are seeing increasing pressure on the land as are areas in Ethiopia, Uganda, and Kenya.

If a pixel experiences an HANPP (% of NPP) value higher than 100%, the NPP needed for the current agricultural demand in the particular pixel exceeds the current

TABLE 4.7
Change in the Spatial Pattern of the Human Appropriation of HANNP as a Proxy for Food Insecurity in 1995 and Projected for 2018 within the Degraded Cultivated Land and All Cultivated Land

Pressure on Land HANPP[a] (% of NPP)	Food Security Threat	Degraded Agricultural Land		All Agricultural Land	
		Area in 1995[b] (km^2)	Area in 2018[c] (km^2)	Area in1995[b] (km^2)	Area in 2018[c] (km^2)
0–25	Very low	795,712	541,504	2,774,144	2,097,472
25–50	Low	229,120	237,440	620,928	756,672
50–75	Moderate	88,832	154,624	270,080	383,872
75–100	High	47,872	85,312	127,296	236,672
>100	Very high	79,232	221,888	186,240	496,640

[a] In cultivated areas of SSA, HANPP is approximately the food appropriation of NPP (FANPP).

[b] Extracted and reclassified from Imhoff et al. (Human Appropriation of Net Primary Productivity as a Percentage of Net Primary Productivity, Socioeconomic Data and Applications Center, 2004b; with permission).

[c] Projected using the actual NDVI slope from Figure 4.4b and an average population growth rate (3% per year).

productivity of the land, thus illustrating a very high threat of food insecurity and dependence on imports. Table 4.7 reveals that such areas will increase over the coming 20 years by about 250%. The areas where pressure on land (HANPP) is high and moderate will increase as well at the expense of those with low and very low HANPP.

4.6 CONCLUSIONS AND RECOMMENDATIONS

It seems reasonable to assume that, when information derived from remote sensing observation over a 20-year time slice suggests a declining biomass production as measured in NDVI, the underlying degradation processes must indeed be rather severe, particularly on agricultural land. Even though the extent of areas that exhibited actually declining NDVIs over the past 20 years of the last century with 10% of the SSA landmass seems relatively modest (Vlek et al., 2008), if added to the 10% that was already claimed to be severely degraded in the late 1980s by the GLOSOD team, the land resources of Africa are indeed dwindling. Moreover, if atmospheric fertilization is taken into account, the human footprint in SSA increases to nearly 30%. Additionally, land degradation may be ongoing at the microscale (patches) level, which is not captured as significant in an 8 × 8 km pixel. As time series of higher-resolution satellites become available, more detailed analysis on a country-by-country basis should better inform about the state of land and soils. In the absence of any instruments for monitoring the rate of land degradation in SSA on the ground, satellite-based systems are the most promising for tracking the state of this vital natural resource on the vast African continent. A systematic research effort should be made to verify the accuracy of the findings reported here and to refine the analytical tool and interpretation of the results.

Land degradation processes vary according to land use. In the forested areas of the humid tropics it would be due to deforestation, which seems to be taking place predominantly in areas with bad to very bad soil and terrain conditions. Overgrazing would be the prime form of land degradation on grasslands, and the greatest impact of this type of mismanagement appears to occur in the arid/semiarid regions and predominantly on land with the better soil and terrain conditions. Both types of land mismanagement have a negative impact on the soil resources, which are deprived of their protective vegetation; the involved practices should be avoided.

The human impact on the productive capacity of agricultural land in SSA is largely related to unsustainable soil management such as elimination of fallows, removal and burning of crop residues, produce exports, and shifts to more demanding crops. The consequences are soil acidification, loss of soil organic matter and nutrients, and soil erosion. Approximately 1 million km^2 appear to be affected, 40% of which comprises the land with inherently good soil and terrain conditions in the most productive areas of SSA, thus threatening food production in the long run. Approximately 65% of this unsustainable land management goes unnoticed, as atmospheric fertilization (CO_2 and NO_x) is compensating some of the depleting processes, so that the actual decline in the NDVI signal on agricultural land is noticeable only on 285,000 km^2 (Vlek et al., 2008).

Finally, it should be noted that land degradation in SSA is taking place against a background of increasing population and deteriorating climate conditions in a food-

insecure part of the world. It is also the only part of the world where fertilizer use has been stagnant over the past 25 years at a value of below 10 kg ha^{-1} yr^{-1}. The persistent decline in NPP induced by mismanagement of agricultural activities against the background of the steady growth of agrarian population (about 3% annually) will likely lead to an increasing pressure on agricultural land, threatening the food security of an additional 250,000 km^2 by the end of the 2010s.

A land resource analysis of the type presented here can provide the basis for identifying areas with common climatic, vegetation, physiographic, and soil and land-use characteristics that appear to be threatened by human-induced land degradation. Immediate adaptation strategies are needed in areas characterized by favorable soil and terrain where population pressure is high and degradation is in full progress. These may involve capital-intensive land conservation measures and fertilizer adoption, because such practices are likely to be profitable in such environments (Kaizzi et al., 2006). In less-endowed environments, farmers may have to rely on more labor-intensive measures such as conservation agriculture (Vlek and Tamene, 2009).

This assessment can only be seen as a first approximation, and the maps and analysis here need extensive verification in the field. The analysis, in essence, is as good as the underlying databases. However, as better data become available, the analysis framework proposed here allows easy substitution of this information and rapid generation of an updated assessment.

REFERENCES

Abubakar, S. M. 1997. Monitoring land degradation in the semi-arid tropics using inferential approach: the Kabomo basin case study, Nigeria. *Land Degrad Dev* 8:311–323.

Achard, F., H. Eva, and P. Mayaux. 2001. Tropical forest mapping from coarse spatial resolution satellite data: production and accuracy assessment issues. *Int J Remote Sens* 22: 2741–2762.

Adam, A. B., R. B. Harrison, R. S. Sletten, B. D. Strahm, E. C. Turnblom, and C. M. Jensen. 2005. Nitrogen-fertilization impacts on carbon sequestration and flux in managed coastal Douglas-fir stands of the Pacific Northwest. *For Ecol Manage* 220:313–325.

Bai, Z. G., D. L. Dent, L. Olsson, and M. E. Schaepman. 2008. Proxy global assessment of land degradation. *Soil Use Manage* 24: 223–234.

Balk, D., and G. Yetman. 2004. *Gridded Population of the World—Version 3 Documentation*. New York, NY: Center for International Earth Science Information Network, Columbia University.

Bartalev, S., A. S. Belward, D. Erchov, and A. S. Isaev. 2003. A new SPOT4-VEGETATION derived land cover map of Northern Eurasia. *Int J Remote Sens* 24:1977–1982.

Beck, C., J. Grieser, and B. Rudolf. 2005. *A New Monthly Precipitation Climatology for the Global Land Areas for the Period 1951 to 2000*, 181–190. DWD, Klimastatusbericht KSB 2004, Offenbach, Germany. ISSN 1437-7691, ISSN 1616-5063 (Internet), ISBN 3-88148-402-7.

Boisvenue, C., and S. W. Running. 2006. Impacts of climate change on natural forest productivity—evidence since the middle of the 20th century. *Glob Change Biol* 12:862–882.

Camberlin, P., N. Martiny, N. Philippon, and Y. Richard. 2007. Determinants of interannual relationships between remote sensed photosynthetic activity and rainfall in tropical Africa. *Remote Sens Environ* 106:199–216.

Cihlar, J., R. Latifovic, J. Beaubien, B. Guindon, and M. Palmer. 2003. Thematic Mapper (TM) based accuracy assessment of a land cover product for Canada derived from SPOT VEGETATION (VGT) data. *Can J Remote Sens* 29:154–170.

Dentener, F. J. 2006. Global maps of atmospheric nitrogen deposition, 1860, 1993 and 2050. Data set. Available online (http://daac.ornl.gov/) from Oak Ridge National Laboratory Distributed Active Archive Center, Oak Ridge, TN.

Eastman, J. R., and M. Fulk. 1993. Long sequence time series evaluation using standardized principal components. *Photogramm Eng Remote Sensing* 59:991–996.

Eklundh, L., and L. Olsson. 2003. Vegetation index trends for the African Sahel 1982–1999. *Geophys Res Lett* 30(8):1430, doi: 10.1029/2002GL016772.

Eswaran, H., R. Almaraz, E. van den Berg, and P. Reich. 1997. An assessment of the soil resources of Africa in relation to productivity. *Geoderma* 77:1–18.

Eswaran, H., R. Lal, and P. F. Reich. 2001a. Land degradation: an overview. In: *Responses to Land Degradation*, ed. E. M. Bridges, I. D. Hannam, L. R. Olderman, F. W. T. Penning de Vries, S. J. Scherr, and S. Sompatpanit. *Proc. of the 2nd International Conference on Land Degradation and Desertification*, KonKaen, Thailand. New Delhi, India: Oxford Press.

Eswaran, H., P. Reich, and F. Beinroth. 2001b. Global desertification tension zones. In: *Sustaining the Global Farm*, ed. D. E. Stott, R. H. Mohtar, and G. C. Steinhardt. Selected papers, 10th International Soil Conservation Organization Meeting, May 24–29, 1999, Purdue University and USDA-ARS National Soil Erosion Research Laboratory.

Evans, J., and R. Geerken. 2004. Discrimination between climate and human-induced dryland degradation. *J Arid Environ* 57(4):535–554.

Fiedler, K., and P. Döll. 2007. Global modelling of continental water storage changes—sensitivity to different climate data sets. *Adv Geosci* 11:63–68.

Field, C. B., J. T. Randerson, and C. M. Malmström. 1995. Global net primary production: combining ecology and remote sensing. *Remote Sens Environ* 51:74–88.

Fischer, G., H. van Velthuizen, M. Shah, and F. O. Nachtergaele. 2002. *Global Agro-Ecological Assessment for Agriculture in the 21st Century: Methodology and Results*, RR-02-02. Laxenburg, Austria: FAO and IIASA.

Fritz, S., E. Bartholome, A. Belward, A. Hartley, H. J. Stibig, E. Eva, P. Mayaux, S. Bartalev, R. Latifovic, S. Kolmert, P. S. Roy, S. Agrawal, B. Wu, W. Xu, M. Ledwith, J. F. Peckel, C. Giri, M. S. Cher, D. E. Badts, R. Tateischi, J. L. Champeaux, and Y. P. Defourn. 2003. *Harmonisation, Mosaicing and Production of the Global Land Cover 2000 Database (Beta Version)*. Publication of the European Commission EUR 20849 EN. Luxembourg: Office for Official Publications of the European Communities.

Giri, C., Z. Zhu, and B. Reed. 2005. A comparative analysis of the Global Land Cover 2000 and MODIS land cover data sets. *Remote Sens Environ* 94(1):123–132.

Galloway et al. 2004. Nitrogen cycles: past, present, and future. *Biogeochemistry* 70:153–226.

GEF. 2006. Global Environmental Facility: protecting the global environment—Africa, http://www.theGEF.org.

Gessler, P. E., O. A. Chadwick, F. Chamran, L. Althouse, and K. Holmes. 2000. Modeling soil–landscape and ecosystem properties using terrain attributes. *SSAJ* 64: 2046–2056.

Grace, J., J. Lloyd, J. McIntyre, A. C. Miranda, P. Meir, H. S. Miranda, C. Nobre, J. Moncrieff, J. Massheder, Y. Malhi, I. Wright, and J. Gash. 1995. Carbon dioxide uptake by an undisturbed tropical rain forest in Southwest Amazonia, 1992 to 1993. *Science* 270:778–780.

Groten, S. M. E., and R. Ocatre. 2002. Monitoring the length of the growing season with NOAA. *Int J Remote Sens* 23(14):1271–1318.

Hagedorn, F., S. Maurer, J. B. Bucher, and R. T. W. Siegwolf. 2005. Immobilization, stabilization and remobilization of nitrogen in forest soils at elevated CO_2: a ^{15}N and ^{13}C tracer study. *Glob Change Biol* 11:1816–1827.

Hellden, U., and C. Tottrup. 2008. Regional desertification: a global synthesis. *Glob Planet Change* 64: 169–176.

Herrmann, S. M., A. Anyamba, and C. J. Tucker. 2005. Recent trends in vegetation dynamics in the African Sahel and their relationship to climate. *Glob Environ Change* 15:394–404.

Huxman, T. E., M. D. Smith, P. A. Fay, A. K. Knapp, M. R. Shaw, M. E. Loik et al. 2004. Convergence across biomes to a common rain-use efficiency. *Nature* 429:651–654.

Ichii, K., Y. Matsui, K. Murakami, Y. Yamaguchi, and K. Ogawa. 2002. Future projections of global environment due to anthropogenic CO_2 emission: analysis from a simplified carbon cycle model and climate coupled model and earth observation satellite data. *J Remote Sens Soc Jpn* 22(5):625–636.

Imhoff, M. L., L. Bounoua, T. Ricketts, C. Loucks, R. Harriss, and W. T. Lawrence. 2004a. Global patterns in human consumption of net primary production. *Nature* 429:870–873.

Imhoff, M. L., L. Bounoua, T. Ricketts, C. Loucks, R. Harriss, and W. T. Lawrence. 2004b. Human Appropriation of Net Primary Productivity as a Percentage of Net Primary Productivity. Data distributed by the Socioeconomic Data and Applications Center (SEDAC): http://sedac.ciesin.columbia.edu/es/hanpp.html, accessed on May 6, 2009.

Kaizzi, C. K., H. Ssali, and P. L. G. Vlek. 2006. Differential use and benefits of velvet bean (*Mucuna pruriens* var. *utilis*) and N fertilizers in maize production in contrasting agro-ecological zones of E. Uganda. *Agric Syst* 88:44–60.

Katyal, J. C., and P. L. G. Vlek. 2000. Desertification—concept, causes and amelioration. ZEF Discussion Paper No. 33. Bonn: Center for Development Research.

Körner, C. 2000. Biosphere responses to CO_2 enrichment. *Ecol Appl* 10:1590–1619.

Kottek, M., J. Grieser, C. Beck, B. Rudolf, and F. Rubel. 2006. World map of the Köppen-Geiger climate classification updated. *Meteorol Z* 15:259–263.

LeBauer, D. S., and K. K. Treseder. 2008. Nitrogen limitation of net primary productivity in terrestrial ecosystems is globally distributed. *Ecology* 89(2):371–379.

Lewis, S. L., G. Lopez-Gonzalez, B. Sonké, K. Affum-Baffoe, T. R. Baker, et al. 2009. Increasing carbon storage in intact African tropical forests. *Nature* 457:1003–1006.

Magnani, F., M. Mencuccini, M. Borghetti, P. Berbigier, F. Berninger, et al. 2007. The human footprint in the carbon cycle of temperate and boreal forests. *Nature* 447:848–850.

Mayaux, P., E. Bartholome, S. Frtiz, and A. Belward. 2004. A new land-cover map of Africa for the year 2000. *J Biogeogr* 31:861–877.

Middleton, N., and D. S. G. Thomas. 1992. *World Atlas of Desertification*, 1st edn. London: Edward Arnold, UNEP.

Millennium Ecosystem Assessment. 2005. *Ecosystems and Human Well-being: Synthesis*. Washington, D.C.: Island Press.

Milich, L., and E. Weiss. 2000. GAC NDVI interannual coefficient of variance (CoV) images: ground truth sampling of the Sahel along north-south transects. *Int J Remote Sens* 21(1):235–260.

Mitchell, T. D., and P. D. Jones. 2005. An improved method for constructing a database of monthly climate observations and associated high-resolution grids. *Int J Climatol* 25:693–712.

Nicholson, S. E., M. L. Davenport, and A. R. Malo. 1990. A comparison of the vegetation response to rainfall in the Sahel and East Africa, using Normalized Difference Vegetation Index from NOAA AVHRR. *Clim Change* 17:209–241.

Norby, R. J., E. H. DeLucia, B. Gielen, C. Calfapietra, C. P. Giardina, et al. 2005. Forest response to elevated CO_2 is conserved across a broad range of productivity. *Proc Natl Acad Sci USA* 102:18052–18056.

Nowak, R. S., D. S. Ellsworth, and S. D. Smith. 2004 Functional responses of plants to elevated atmospheric CO_2—do photosynthetic and productivity data from FACE experiments support early predictions? *New Phytol* 162:253–280.

O'Connor, T. G., L. M. Haines, and H. A. Snyman. 2001. Influence of precipitation and species composition on phytomass of a semi-arid African grassland. *J Ecol* 89:850–860.

Oldeman, L. R., R. T. A. Hakkeling, and W. G. Sombroek. 1990. *World Map of the Status of Human-Induced Soil Degradation: An Explanatory Note*, 34 pp. Wageningen: ISRIC.

Olsson, L. 1993. On the causes of famine: drought, desertification and market failure in the Sudan. *Ambio* 22:395–403.

Olsson, L., L. Eklundh, and J. Ardö. 2005. A recent greening of the Sahel: trends, patterns and potential causes. *J Arid Environ* 63:556–566.

Park, S. J., K. McSweene, and B. Lowery. 2001. Prediction of soils using a process based terrain characterization. *Geoderma* 103:249–272.

Prince, S. D., E. Brown De Colstoun, and L. L. Kravitz. 1998. Evidence from rain-use efficiency does not indicate extensive Sahelian desertification. *Glob Change Biol* 4:359–379.

Prince, S. D., and S. Goward. 1995. Global primary production: a remote sensing approach. *J Biogeogr* 22:815–835.

Reay, D. S., F. Dentener, P. Smith, J. Grace, and R. Feely. 2008. Global nitrogen deposition and carbon sinks. *Nat Geosci* 1:430–437.

Reich, R., H. Eswaran, S. Kapur, and E. Akca. 2001. *Land Degradation and Desertification in Desert Margins*. Washington, D.C.: USDA Natural Resources Conservation Service.

Reynolds, J. F., and D. M. S. Smith. 2002. *Global Desertification—Do Humans Cause Deserts?* Dahlem Workshop Report 88. Berlin: Dahlem University Press.

Safriel, U. N. 2007. The assessment of global trends in land degradation. In: *Climate and Land Degradation*, ed. M. V. K. Sivakumar and N. Ndiang'ui, 1–38. Berlin: Springer Verlag.

Sheng, T. C. 1990. *Watershed Management Field Manual: Watershed Survey and Planning*. FAO Conservation Guide 13/6. Rome, Italy: FAO.

Symeonakis, E., and N. Drake. 2004. Monitoring desertification and land degradation over sub-Saharan Africa. *Int J Remote Sens* 25(3):573–592.

Tamene, L., S. J. Park, R. Dikau, and P. L. G. Vlek. 2006. Analysis of factors determining sediment yield variability in the highlands of northern Ethiopia. *Geomorphology* 76:76–91.

Thiam, A. K. 2003. The causes and spatial pattern of land degradation risk in southern Mauritania using multi-temporal AVHRR-NDVI imagery and field data. *Land Degrad Dev* 14:133–142.

Tucker, C. J., H. E. Dregne, and W. W. Newcombe. 1991. Expansion and contraction of the Sahara desert from 1980 to 1990. *Science* 253:299–301.

Tucker, C. J., and S. E. Nicholson. 1999. Variations in the Size of the Sahara Desert from 1980 to 1997. *Ambio* 28:587–591.

Tucker, C. J., J. E. Pinzon, M. E. Brown, D. A. Slayback, E. W. Pak, R. Mahoney, E. F. Vremote, and N. El Saleous. 2005. An extended AVHRR 8-km NDVI data set compatible with MODIS and SPOT Vegetation NDVI Data. *Int J Remote Sens* 26 (20):4485–4498.

USGS. 2004. *Shuttle Radar Topography Mission, 30 Arc Second Resolution*. Global Land Cover Facility, University of Maryland, College Park, Maryland, February 2000. (http://glcf.umiacs.umd.edu/data/srtm/).

Vlek, P. L. G. 2005. *Nothing Begets Nothing. The Creeping Disaster of Land Degradation*. Bonn: United Nations University, Institute for Environment and Human Security.

Vlek, P. L. G., G. Rodríguet-Kuhl, and R. Sommer. 2003. Energy use and CO_2 production in tropical agriculture and means and strategies for reduction or mitigation. *Environ Dev Sustainability* 6:213–233.

Vlek, P. L. G., Q. B. Le, and L. Tamene. 2008. *Land Decline in Land-Rich Africa: A Creeping Disaster in the Making*. Rome: CGIAR Science Council Secretariat.

Vlek, P. L. G., and L. Tamene. 2009. Conservation agriculture: why? In *Lead Papers, 4th World Congress on Conservation Agriculture*, New Delhi, India, pp 10–20.

Weiss, E., S. E. Marsh, and E. S. Pfirman. 2001. Application of NOAA AVHRR NDVI time series to assess changes in Saudi Arabia's rangelands. *Int J Remote Sens* 22(6):1005–1027.

Wessels, K. J., S. D. Prince, J. Malherbe, J. Small, P. E. Frost, and D. van Zyl. 2007. Can human-induced land degradation be distinguished from the effects of rainfall variability? A case study in South Africa. *J Arid Environ* 68:271–279.

Wilson, J., and C. Gallant. 2000. Digital terrain analysis. In *Terrain Analysis: Principles and Applications*, ed. J. P. Wilson and J. C. Gallant. New York, NY: Wiley & Sons.